


iNOS/Arginase-I expression in the pulmonary tissue over time during *Cryptococcus gattii* infection

Innate Immunity
2020, Vol. 26(2) 117–129
© The Author(s) 2019
Article reuse guidelines:
sagepub.com/journals-permissions
DOI: 10.1177/1753425919869436
journals.sagepub.com/home/ini


Patrícia Kellen Martins Oliveira-Brito^{1,*},
Caroline Patini Rezende^{2,*}, Fausto Almeida²,
Maria Cristina Roque-Barreira¹ and
Thiago Aparecido da Silva¹ 

Abstract

Inhalation of *Cryptococcus gattii* yeasts (causing cryptococcosis) triggers an anti-cryptococcal immune response initiated by macrophages, neutrophils or dendritic cells, and the iNOS expressed by various cells may regulate the function and differentiation of innate and adaptive immune cells. Here, we evaluated the effect of progression of *C. gattii* infection on the host innate immune response. *C. gattii* infection in BALB/c mice spreads to several organs by 21 d post infection. The numbers of neutrophils and lymphocytes in the peripheral blood of *C. gattii*-infected mice were remarkably altered on that day. The frequency of CD11b⁺ cells and cell concentrations of CD4⁺ and CD8⁺ T cells was significantly altered in the pulmonary tissue of infected mice. We found a higher frequency of CD11b⁺/iNOS⁺ cells in the lungs of infected mice, accompanied by an increase in frequency of CD11b⁺/Arginase-I⁺ cells over time. Moreover, the iNOS/Arginase-I expression ratio in CD11b⁺ cells reached its lowest value at 21 d post infection. In addition, the cytokine micro-environment in infected lungs did not show a pro-inflammatory profile. Surprisingly, iNOS knock-out prolonged the survival of infected mice, while their pulmonary fungal burden was higher than that of infected WT mice. Thus, *C. gattii* infection alters the immune response in the pulmonary tissue, and iNOS expression may play a key role in infection progression.

Keywords

Cryptococcus gattii, host immune response, iNOS, arginase-I, pulmonary tissue

Date Received: 1 May 2019; revised: 14 July 2019; accepted: 22 July 2019

Introduction

Cryptococcus gattii, a causative agent of cryptococcosis, is an emerging fungal pathogen that preferentially infects the lungs and CNS of immunocompetent individuals.¹ It preferentially infects the pulmonary tissue, which is supported by animal studies that associate mortality with pulmonary infection.² Following the inhalation of *C. gattii* yeast or desiccated basidiospores, lung-resident macrophages initiate an anti-cryptococcal immune response. Infiltrating macrophages can act in both fungal clearance and dissemination, which have been described as two phenotypes: M1 (classically activated macrophages) and M2 (alternatively activated macrophages), respectively.^{3,4} These macrophage

phenotypes are defined by expression of markers: M1 markers include inducible NO synthase (iNOS or iNOS2), while M2 markers include arginase-I

¹Department of Cell and Molecular Biology and Pathogenic Bioagents, Ribeirão Preto Medical School, University of São Paulo, Brazil

²Department of Biochemistry and Immunology, Ribeirão Preto Medical School, University of São Paulo, Brazil

*These authors contributed equally to this work.

Corresponding author:

Thiago Aparecido Da Silva, Department of Cell and Molecular Biology and Pathogenic Bioagents, Ribeirão Preto Medical School, University of São Paulo, Avenida Bandeirantes 3900, Ribeirão Preto, 14049-900, São Paulo, Brazil.

Emails: sthiagoap@gmail.com; sthiagoap@usp.br



(Arg-1), found in inflammatory zone 1 (Fizz1), and chitinase-like molecule (Ym1).^{5,6}

The role of iNOS expressed by macrophages is critical in the balance between M1 and M2 subsets, because iNOS regulates the expression of hallmark genes in M1 macrophages and modulates the production of pro-inflammatory cytokines.^{7,8} On the other hand, Arg-1 expressed by macrophages plays a pivotal role in the regulation of the immune response, mostly through competition between iNOS and Arg-1 for the intracellular arginine, resulting in the protection of tissue against injury in response to inflammation.⁹ iNOS and Arg-1 are expressed by a variety of cells, and the effector activity of immune cells may be regulated by iNOS.^{10–12} Previous studies have demonstrated that iNOS expression can negatively regulate the differentiation of effector dendritic cells (DCs),¹³ and iNOS also acts as a mediator in the suppressive function of myeloid-derived suppressor cells.¹⁴ These findings evidence a regulatory function of iNOS expression on immune cells modulating the immune response against pathogens. In the context of *Cryptococcus neoformans* infection, iNOS activity was required to generate a primary immune response, while iNOS expression was not essential for the development of secondary immunity to *C. neoformans* infection.¹⁵

Previous studies have reported a protective effect of IFN- γ and Th1 cells during *C. neoformans* infection.^{16,17} Th17 immunity has been shown to collaborate with the protective Th1-type anti-cryptococcal immune response.^{18,19} However, Th1 and Th17 responses in the lungs are impaired during *C. gattii* infection, owing to multiple factors: (a) *C. gattii* fails to provoke the migration of neutrophils in the lungs, (b) lower levels of pro-inflammatory cytokines in the lung and higher levels of IL-13 in response to *C. gattii* infection and (c) attenuation of DCs, impairing chemokine expression associated with the induction of the Th1 immune response.^{20,21} Interestingly, the major pro-inflammatory cytokine, IFN- γ , associated with an overall protective Th1 immune response, failed to potentiate the phagocytic and microbicide activity of macrophages in the presence of *C. gattii*.^{22,23} In this line, reactive oxygen species (ROS), which play a critical role in the microbicidal activity of phagocytic cells, favour the growth of *C. gattii* strain R265.^{24,25} These findings support the ability of *C. gattii* to infect both immunocompromised and immunocompetent hosts.

In the current study, we evaluated the effects of the progression of *C. gattii* infection on the host immune response. The plasticity of iNOS/Arg-1 expression in the lungs was also studied. The frequency of CD11b⁺ cells in pulmonary tissue was higher in *C. gattii*-infected mice than in uninfected mice in all periods studied, and the concentrations of CD4⁺ and CD8⁺

T cells were significantly increased on day 21 post infection relative to uninfected mice. We found that the cell concentration of CD11b⁺/Arg-1 cells increased over time during infection and reached levels close to CD11b⁺/iNOS on day 21 post infection. Interestingly, the *C. gattii* burden in the lungs of knock-out (KO) mice for iNOS was higher relative to WT mice. However the absence of iNOS prolonged the survival of mice infected with *C. gattii*.

Materials and methods

Animals

Male BALB/c, C57BL/6 and iNOS KO (C57BL/6 genetic background) mice, 6–8 wk old, were acquired from the animal house of the Campus of Ribeirão Preto, University of São Paulo (Ribeirão Preto, São Paulo, Brazil). Animals were maintained under standard housing conditions in the Department of Cell and Molecular Biology and Pathogenic Bioagents of the Ribeirão Preto Medical School, University of São Paulo, under optimised hygienic conditions. All animal experiments were approved by the Committee on Ethics in Animal Research of the Ribeirão Preto Medical School at the University of São Paulo and were conducted in accordance with the Ethical Principles in Animal Research adopted by the Brazilian College of Animal Experimentation (protocol 204/2016).

Fungicidal activity of AMJ2-C11 cell line in the presence of L-NG-monomethyl-L-arginine acetate

The alveolar macrophage cell line was routinely grown in DMEM (Gibco®; Life Technologies, Carlsbad, CA) supplemented with 10% FBS, 4 mM L-glutamine, 4500 mg/l Glc, 5 mM HEPES and antibiotics in a humidified 5% CO₂ atmosphere at 37°C. The AMJ2-C11 cell line was kindly provided by Dr Ana Marisa Fusco-Almeida (Department of Clinical Analysis, Laboratory of Clinical Mycology, Faculty of Pharmaceutical Sciences, São Paulo State University-UNESP, Araraquara-SP, Brazil).

AMJ2-C11 macrophages (5×10^5 /ml) were incubated with L-NG-monomethyl-L-arginine acetate (L-NMMA; 1 mM) or medium alone (negative control) for 4 h, and these cells were infected with *C. gattii* yeasts (yeast-to-macrophage ratio of 1:100). After 24 h of incubation, the monolayer culture was detached and mixed with supernatant to quantify the growth of *C. gattii* by the CFU assay.

C. gattii infection and survival analysis

C. gattii strain R265 (VGII molecular genotype) was recovered from 25% glycerol stocks stored at -80°C and plated on Sabouraud dextrose agar. After 24 h of incubation at 30°C , one loopful from a single colony was inoculated in Sabouraud dextrose broth and grown for 24–30 h at 30°C with constant shaking. Yeast were harvested by centrifugation at $7500g$ for 10 min at 25°C , washed in sterile PBS and counted using China ink in a Neubauer chamber.

Animals were anaesthetised with ketamine (150 mg/kg of body mass) and xylazine (7.5 mg/kg of body mass) prior to intra-nasal inoculation of *C. gattii* (10^3 – 10^6 yeast/mice). The control group received intra-nasal PBS alone. The survival of mice was assessed daily over 47 d to create the survival curve. For other assays, an inoculum of 10^4 *C. gattii* per mouse was used, and the control group received PBS alone. Animals were euthanized on d 7, 14 and 21 post infection to collect whole blood, lungs, brain, liver, spleen, heart and kidneys aseptically. The KO mice were euthanized on d 14 post infection for fungal burden analysis.

Fungal burden

Fungal burden was assessed in the blood, lungs, brain, liver, spleen, heart and kidney homogenates. Tissue homogenates were diluted in sterile PBS buffer (pH 7.2), and 50 μl aliquots were plated on Sabouraud dextrose agar. After 48 h at 30°C , the number of CFU was determined as CFU/mg organ mass, as described by Almeida et al.²⁶

Measurement of biochemical markers

Plasma levels of glutamic oxaloacetic transaminase (GOT), glutamic pyruvic transaminase (GPT), amylase and creatinine were measured with a commercial colorimetric assay (Labtest, Lagoa Santa, Brazil). Concentrations were measured by absorbance using a spectrophotometer (Power Wave-X microplate reader; BioTek Instruments, Inc., Winooski, VT) according to the manufacturer's instructions.

Leucogram in the peripheral blood

Peripheral blood was collected by cardiac puncture. Blood was diluted 1:20 in Turk's solution, and the total leucocyte count was estimated using a Neubauer chamber. Mononuclear and granulocytic cells from the blood smear were quantified under a light microscope with an oil immersion (100 \times) objective after panoptic staining. Total leucocyte, lymphocyte, neutrophil and monocyte counts were expressed as leucocytes/mm³.

The determinations of relative numbers of lymphocyte, neutrophil and monocyte counts are expressed as percentages. In both leucocyte analyses, the procedures were performed as described by Oliveira-Brito et al.²⁷

Pulmonary leucocyte isolation

Lung tissues of uninfected and infected mice were perfused with sterile $1\times$ PBS on day 0, 7, 14 and 21 post infection. The lungs were removed and fragmented with scissors to 1-mm chunks, placed in falcon tubes with RPMI 1641 medium (2 ml) and subjected to digestion in RPMI 1640 plus 10 U/ μl collagenase type IV (Sigma–Aldrich, St Louis, MO) and 20 $\mu\text{g}/\text{ml}$ of Type IV DNase I at 37°C for 45 min. The reaction was stopped by adding 1 ml heat-inactivated FBS. The digested tissues were successively filtered (40 μm ; Thermo Fisher Scientific, Durham, NC) and washed with PBS. Erythrocytes were depleted with lysis buffer (nine parts 0.16 M ammonium chloride and one part 0.17 M Tris–HCl; pH 7.5) for 5 min at 4°C , followed by the addition of a 10-fold excess of PBS. The leucocytes were centrifuged (300 g) for 10 min, washed twice with PBS and suspended in PBS plus 10% heat-inactivated FBS. The live cell count was determined using trypan blue dye exclusion in a haemocytometer.

Flow cytometry using pulmonary leucocytes

Aliquots of 1×10^6 cells from each mouse were assayed to phenotype T cells and CD11b⁺ populations within iNOS⁺ cells and Arg-1⁺ cells by flow cytometry. Pulmonary leucocytes were incubated with anti-CD4 FITC (20 $\mu\text{g}/\text{ml}$; clone H129.19) plus anti-CD3 PE (20 $\mu\text{g}/\text{ml}$; clone 145-2C11), or anti-CD8 FITC (20 $\mu\text{g}/\text{ml}$; clone 53-6.7) plus anti-CD3 PE to quantify CD4⁺ and CD8⁺ T cells, respectively. After 45 min, the cells were washed twice with PBS and analysed by flow cytometry (Guava easyCyte, Guava Technologies; Millipore, Hayward, CA). The pulmonary leucocytes were incubated with anti-CD11b PE (20 $\mu\text{g}/\text{ml}$; clone M1/70) Ab for 45 min at 4°C and washed twice with PBS before being fixed and permeabilised with a Fixation/Permeabilization Solution Kit (Cytofix/CytopermTM; BD Biosciences, Franklin Lakes, NJ) for 20 min at 4°C . Then, they were washed with permeabilisation wash buffer (BD Biosciences). Cells were incubated with murine anti-iNOS (1:200; clone 4E5) or rabbit anti-Arg-1 (1:100; clone 24HCLC) Ab for 45 min at 4°C . Cells were washed and incubated with anti-mouse IgG-biotin Ab (1:100) or anti-rabbit IgG-biotin Ab (1:100) for 45 min at 4°C . Afterwards, the cells were washed and incubated with streptavidin-FITC conjugate (1:100) for 45 min at 4°C and then

analysed by flow cytometry. The CD11b⁺ cells were gated to distinguish the positive cells for iNOS or Arg-1 expression, and the data were used to calculate the percentage, cell concentration and fluorescence intensity of CD11b⁺/iNOS⁺ and CD11b⁺/Arg-1⁺.

Cytokine measurement

Lungs collected from infected mice were homogenised in 1 ml sterile PBS and centrifuged at 3200 g for 10 min at 4°C. The supernatants were used for the measurement of IL-12p40, TNF- α , IFN- γ , IL-10 and IL-17 levels by ELISA according to the manufacturer's protocol using Ab pairs purchased from BD Biosciences (Pharmingen, San Diego, CA), as previously described.^{26,27} Concentrations were determined relative to standard curves prepared from recombinant murine cytokines. Absorbances were read at 450 nm in a PowerWave X microplate scanning spectrophotometer (BioTek Instruments, Inc.). The levels of cytokines are expressed as picograms per milligram of tissue.

Quantitative RT-PCR

Total RNA was extracted from the lungs with TRIzol reagent according to the manufacturer's instructions. Reverse transcription to produce cDNA from oligo d (T) primers was performed using the ImProm-IITM Reverse Transcription System (Promega Corp., Fitchburg, WI). PCR was performed using EVA Green (Bio-Rad Laboratories, Hercules, CA) on a Bio-Rad CFX96 Real-Time Detection System in 10 μ l reaction volumes under the following conditions: 95°C for 30 s, then 40 cycles of 95°C for 5 s and 60°C for 5 s. Quantification of gene expression was performed by the $\Delta\Delta$ Ct method relative to a β -actin endogenous control. The specific gene primers used for quantitative RT-PCR of macrophage polarisation markers were: β -actin (F-CCTAAGGCCAACCGTG AAAA; R GAGGCATACAGGGACAGCACA), iNOS2 (F-CCGAAGCAAACATCACATTCA; R-GGTCTAAAGGCTCCGGGCT), Arg-1 (F-GTTCC CAGATGTACCAGGATTC; R-CGATGTCTTTGG CAGATATGC) and Yml (F-TCACAGGTCTGG CAATTCTTCTG; R-ACTCCCTTCTATTGGCCTG TCC). This analysis was performed as previously described.^{28–30}

Statistical analysis

Results are presented as means \pm SEM or means \pm SD. All data were analysed using GraphPad Prism v6.0 (GraphPad Software, San Diego, CA). The normality and homogeneity of variance of all statistical determinations were analysed by the Kolmogorov–Smirnov test. Student's *t*-test was applied to experiments with

two groups, and ANOVA followed by Bartlett's tests was applied to experiments with three or more groups when the samples had Gaussian distributions. For data sets with a non-normal distribution, the Mann–Whitney test was applied to experiments with two groups, and the Kruskal–Wallis test was used for experiments with three or more groups. Differences between the means of groups were evaluated by one-way ANOVA followed by Tukey's multiple comparisons test or Kruskal–Wallis test followed by Dunn's multiple comparisons test. Survival curves were analysed by log-rank (Mantel–Cox) tests. Differences at $P < 0.05$ were considered statistically significant. All assays were performed independently in triplicate, and five mice were used for each group in all experiments.

Results

Systemic evaluation of fungal burden and biochemical markers after *C. gattii* intra-nasal inoculation

Since host-pathogen interactions during *C. gattii* infection have not been fully studied, we evaluated biochemical and immunological changes during experimental murine infection. BALB/c mice were inoculated intranasally with 10³, 10⁴, 10⁵ and 10⁶ *C. gattii* yeasts, with the negative control group receiving vehicle instead of fungal suspension. Mouse survival was monitored daily for 7 wk post infection, and the survival curves of the experimental groups were different for various inoculum. By 5 wk post infection, all animals in the 10⁵ or 10⁶ groups had died, whereas complete mortality was observed at 6 wk post infection in the groups inoculated with 10⁴ yeasts. Groups inoculated with 10³ yeasts exhibited 60% mortality at the end of the 7-wk observation period (Figure 1a). The mice infected with 10⁴ yeasts were monitored for 3 wk and were euthanized randomly each wk. The lungs of the animals were examined for fungal burden by CFU, which showed a 10-fold increase after each wk post infection (Figure 1b). The CFU assay was also used to detect the presence of *C. gattii* in multiple organs of the infected mice each wk to measure the extent of fungal dissemination in the heart, liver, kidney, brain and spleen. At the end of the first wk, about 20% of the animals presented with *C. gattii* in the liver, kidney and brain, whereas at the end of the second wk, its presence varied from 27% to 48% of mice, varying by organ. At 3 wk post infection, 100% of mice had *C. gattii* in the spleen and brain, while the heart, liver and kidney were affected in 80–95% of mice (Table 1). Fungus was also detected in the blood of 68% of the animals by the

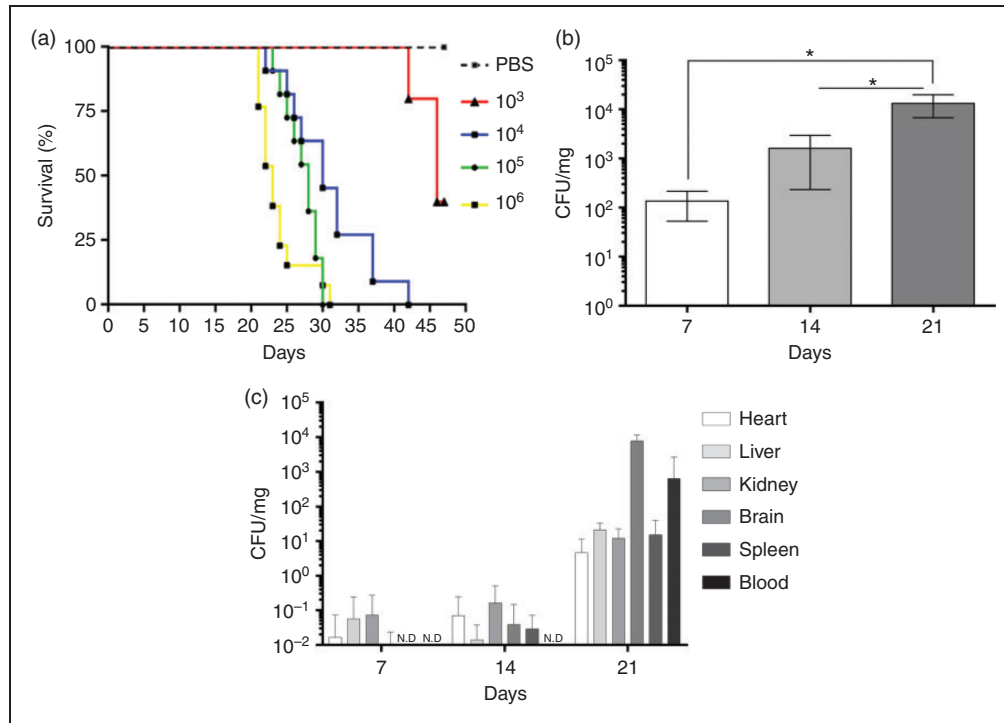


Figure 1. Mouse survival after *C. gattii* infection and the fungal burden in multiple organs. (a) Survival of BALB/c mice after intra-nasal (i.n.) inoculation of 10^3 , 10^4 , 10^5 or 10^6 *C. gattii* yeasts and a control group that received PBS via the intra-nasal route. The survival curve was analysed by a log-rank (Mantel–Cox) test. The differences were considered significant when $*P < 0.05$. (b and c) Fungal burden in infected BALB/c mice. (b) Fungal burden in lung. (c) Fungal burdens in organ homogenates and whole blood on d 7, 14 and 21 post infection. Results are expressed (mean \pm SD) as CFU/mg, CFU/ml or not detected (N.D.).

Table 1. Percentage of infected organs over time during *C. gattii* infection.

Organs	7 dpi	14 dpi	21 dpi
	Mean \pm SD	Mean \pm SD	Mean \pm SD
Heart	7.14 \pm 10.10	28.56 \pm 40.39	80.00 \pm 28.28
Liver	20.00 \pm 0.00	27.14 \pm 18.19	100.00 \pm 0.00
Kidney	14.28 \pm 20.19	48.56 \pm 12.11	100.00 \pm 0.00
Brain	20.00 \pm 0.00	30.00 \pm 42.43	95.00 \pm 7.07
Spleen	0.00 \pm 0.00	38.56 \pm 26.25	90.00 \pm 14.14
Blood	0.00 \pm 0.00	0.00 \pm 0.00	68.33 \pm 2.36

dp: d post infection.

third wk (Table 1). *C. gattii* burden increased in all organs analysed over time during infection, and at 3 wk post infection, the fungal burden was higher in the brain and blood (Figure 1c). These results provide new insights into the progression and dissemination of intra-nasal infection.

Because *C. gattii* dissemination can have systemic effects, we measured the biochemical markers for hepatic, pancreatic and renal dysfunction in the plasma samples. GOT, GPT, amylase and creatinine were evaluated in samples collected from BALB/c mice on d 7, 14 and 21 post infection. Interestingly,

the plasma levels of GOT, GPT, amylase and creatinine in the infected mice did not differ significantly from those of uninfected mice at any of the time points analysed (data not shown). In spite of the statistical difference, the levels of biochemical markers were within normal ranges. Our results indicate that intra-nasal inoculation of 10^4 *C. gattii* yeasts does not significantly alter these biochemical parameters.

C. gattii intra-nasal inoculum causes an alteration in leucogram of the peripheral blood

During our analysis of systemic manifestations of *C. gattii* infection, we performed leucograms on peripheral blood samples collected on d 7, 14 and 21 post infection and compared the results to those from uninfected mice. There was no significant alteration in the total leucocyte count (Figure 2a). Moreover, the absolute number of lymphocytes in mice infected with *C. gattii* decreased on d 21 post infection (Figure 2b) relative to uninfected mice. However, BALB/c mice did not exhibit any alteration in the absolute number of neutrophils and monocytes throughout the infection period (Figure 2c and d). The relative frequencies of leucocytes from uninfected mice were consistent over all periods studied. However, the relative frequencies of

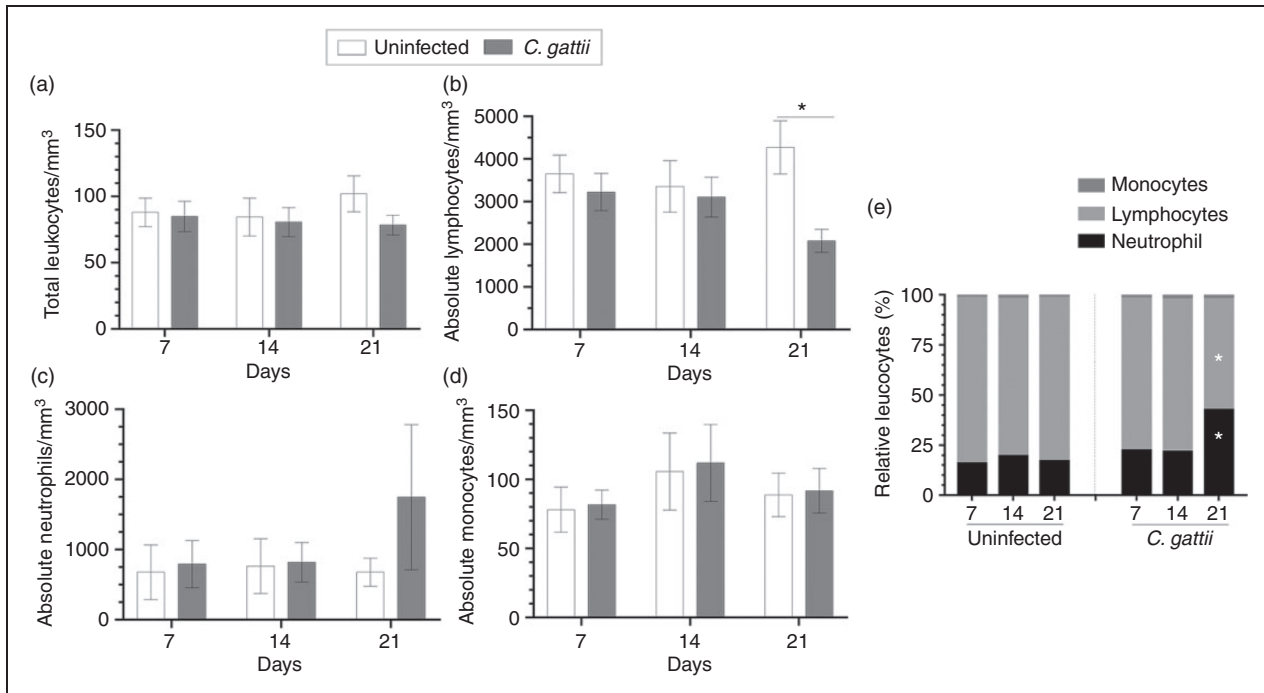


Figure 2. Leucocyte count in the peripheral blood of BALB/c mice infected with *C. gattii*. (a) Total leucocyte, (b) absolute number of lymphocyte, (c) absolute number of neutrophil and (d) absolute number of monocyte counts (leucocytes/mm³) were measured on d 7, 14 and 21 post infection. (e) The relative leucocytes are expressed as percentages. The animals receiving PBS were considered as negative controls (uninfected mice). The values are expressed as means \pm SD. Differences were considered significant at $*P < 0.05$ relative to uninfected controls.

leucocytes from infected mice showed a reduction in the relative lymphocyte count and an increase in the relative neutrophil count on d 21 post infection (Figure 2e). Therefore, *C. gattii* infection is associated with alterations in the absolute number and/or relative frequencies of lymphocytes and neutrophils in the peripheral blood on d 21 post infection.

Persistence of high levels of CD11b⁺ cells in the lungs of C. gattii-infected mice in all period of infection

The measurement of the frequency and cell concentration of leucocytes, such as CD11b⁺ and T cells, in the lungs of mice infected with *C. gattii* was performed by flow cytometry. Pulmonary leucocyte suspensions from *C. gattii*-infected mice and uninfected mice were incubated with anti-CD11b Ab. We observed that the frequencies of CD11b⁺ cells of infected mice were significantly increased at 7, 14 and 21 d post infection relative to those of uninfected mice (Figure 3a). In addition, the percentages and cell concentrations of CD4⁺ T and CD8⁺ T cells were evaluated, which did not differ between infected and uninfected mice (Figure 3b and d). Otherwise, the concentrations of CD4⁺ T and CD8⁺ T cells in pulmonary leucocytes

of infected mice significantly increased on d 21 post infection relative to those of uninfected mice (Figure 3c and e). These findings show that *C. gattii* infection induces an early migration of CD11b⁺ cells into the lungs, while T cells infiltrate later in the infection.

We hypothesised that the cytokine micro-environment in the pulmonary tissue might be drastically altered in *C. gattii*-infected mice due to an imbalance of pro- and anti-inflammatory responses. We therefore measured the IL-12p40, IFN- γ , TNF- α , IL-17 and IL-10 levels in lung homogenates at d 7, 14 and 21 post infection. We did not observe a significant change in pro-inflammatory cytokine levels over this time period (Figure 4a-d). However, IL-10 levels were significantly lower in infected mice than in uninfected controls on d 21 post infection (Figure 4e). Therefore, the reduction of anti-inflammatory cytokine levels, IL-10, in the lungs after infection may be associated with the differentiation and migration of CD11b⁺ cells in the lungs.

Plasticity of iNOS/Arg-1 expression in the lungs during C. gattii infection

We investigated the relative expression of mRNAs encoding the iNOS (M1 macrophages) and Arg-1 and Ym-1 (M2 macrophages) in pulmonary tissue of

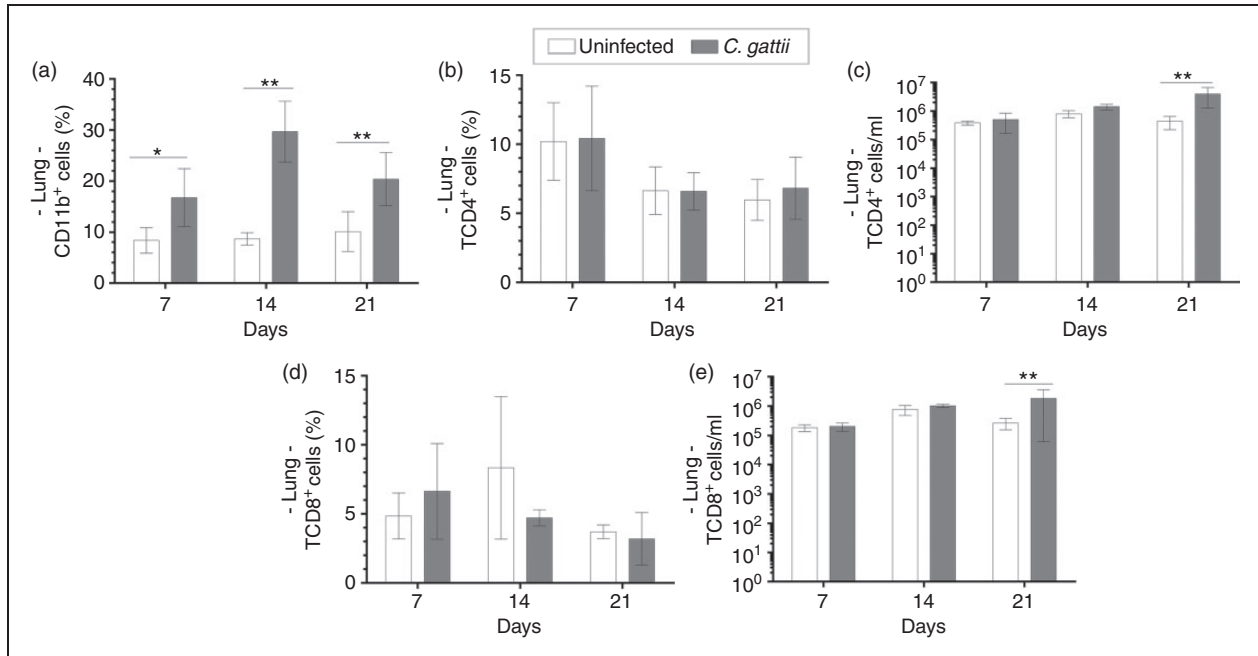


Figure 3. Relative frequency of TCD4⁺ and TCD8⁺ cells in the lung tissue of infected mice. Frequency and/or cell concentration of (a) CD11b⁺, (b and c) CD4⁺ T cells and (d and e) CD8⁺ T cells by flow cytometry on d 7, 14 and 21 post infection. Animals receiving PBS were considered negative controls (uninfected mice). Results are expressed as percentages and represent the mean \pm SD. Differences were considered significant when * $P < 0.05$ and ** $P < 0.01$ relative to uninfected controls.

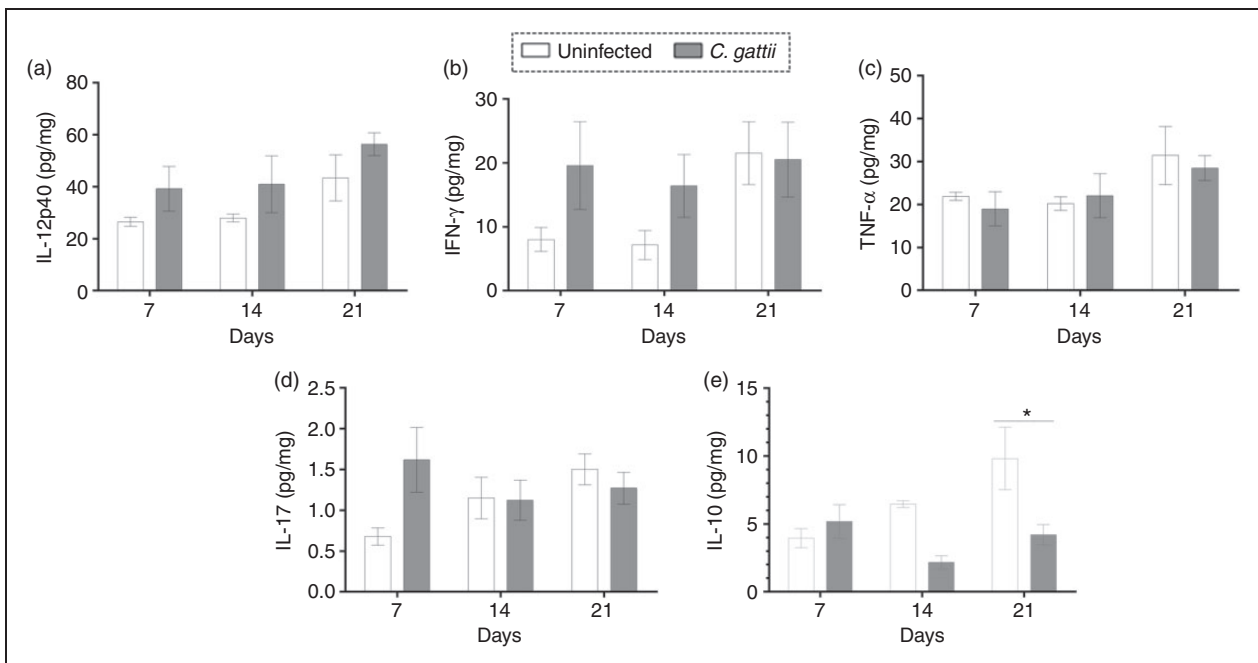


Figure 4. Cytokine levels in the lungs of BALB/c mice during *C. gattii* infection. Lung homogenates of BALB/c infected mice were assayed for (a) IL-12p40, (b) IFN- γ , (c) TNF- α , (d) IL-17 and (e) IL-10 by ELISA on d 7, 14 and 21 post infection. The cytokine concentration was normalised per organ mass and is expressed in picograms per milligram of tissue. The injection of PBS alone (uninfected mice) was used for the control group. Data are shown as the mean \pm SD. Differences were considered significant at * $P < 0.05$ relative to uninfected controls.

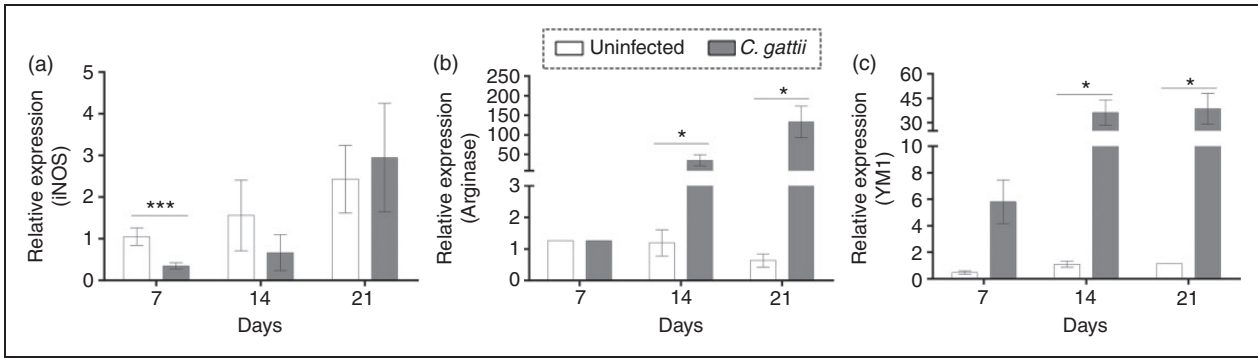


Figure 5. Relative expression of macrophage polarisation markers in the pulmonary tissue of BALB/c mice infected with *C. gattii*. Relative expression levels of (a) iNOS, (b) arginase-I and (c) Ym-1 RNAs determined by quantitative RT-PCR, normalised to β -actin expression. The levels of the relative expression were compared between infected mice and the control group (uninfected). Results are expressed as means \pm SD. Differences were considered significantly different at * $P < 0.05$ and *** $P < 0.001$ relative to uninfected controls.

infected and uninfected mice. The relative expression of iNOS was reduced by infection at 7 d post infection (Figure 5a), while the relative expression of Arg-1 and Ym-1 was increased at 14 and 21 d after infection (Figure 5b and c). The relationship between relative expression of iNOS and Arg-1 was evaluated in CD11b⁺ cells located in the lungs by flow cytometry. CD11b⁺ cells in the lungs include interstitial macrophages, monocytes and polymorphonuclear cells.³¹ Previously to *C. gattii* infection, the prevalence of CD11b⁺/iNOS⁺ cells in the lungs of BALB/c mice was significantly higher compared to CD11b⁺/Arg-1⁺ cells (Figure 6g–i). We found that the fold-change in percentage of CD11b⁺/iNOS⁺ cells and CD11b⁺/Arg-1⁺ cells, as well as their cell concentrations, were significantly higher in the lungs of infected mice relative to uninfected controls at d 14 and/or 21 post infection (Figure 6a and b and d and e). To determine the prevalence of CD11b⁺/iNOS⁺ cells over CD11b⁺/Arg-1⁺ cells, we calculated the frequency and concentrations of these cells over time during infection. We observed that the percentage of CD11b⁺/Arg-1⁺ cells increased on d 14 and 21 post infection (Figure 6g), but the concentration of these cells was lower than that of CD11b⁺/iNOS cells at 7 and 14 d post infection (Figure 6h). However, the CD11b⁺/Arg-1⁺ cell concentration reached levels close to that of CD11b⁺/iNOS⁺ cells by d 21 post infection (Figure 6h). The iNOS/Arg-1 expression ratio was lowest at 21 d post infection (Figure 6i). Thus, the iNOS/Arg-1 expression in CD11b⁺ pulmonary cells dynamically changes during infection.

Absence of iNOS improves the survival of *C. gattii*-infected mice

We showed that over the course of *C. gattii* infection in mice, there was a prevalence of CD11b⁺/iNOS cells in

pulmonary tissue mainly at 7 and 14 d post infection. This cell subset is relevant to the control of cryptococcosis. Initially, the inhibition of iNOS of alveolar macrophage cell line (AMJ2-C11) was performed previously to *C. gattii* infection, and the cells treated with iNOS inhibitor did not reduce the proliferation of *C. gattii* compared to untreated cells (Figure 7a). Therefore, we infected homozygous mutant KO mice for the major inflammatory mediator, iNOS (iNOS KO), with *C. gattii* and the pulmonary fungal burden in these mice was compared to that in control C57BL/6 mice at d 14 post infection. The absence of iNOS resulted in a significantly higher burden in the lungs relative to WT control mice (Figure 7b), but the difference between them was less than a log unit. Surprisingly, the survival curve of *C. gattii*-infected mice demonstrated that the lack of iNOS contributed to higher survival, but it did not prevent the death of the mice (Figure 7c). Thus, while pulmonary fungal growth is impaired by iNOS activity, survival was prolonged in the absence of iNOS (Figure 7).

Discussion

The effect of progression of *C. neoformans* infection on the host immune response is well studied concerning knowledge about *C. gattii* strain R265. Considering the global health impact of cryptococcosis caused by *C. gattii* due its ability to infect both immunocompetent and immunocompromised individuals, we explored the host immunity profile, primarily in pulmonary tissue, during *C. gattii* infection. Initially, we observed that intra-nasal infection induced an alteration in the absolute number and relative frequency of lymphocytes and neutrophils in the peripheral blood. However, the biochemical parameters were not significantly modified. We also observed a consistent

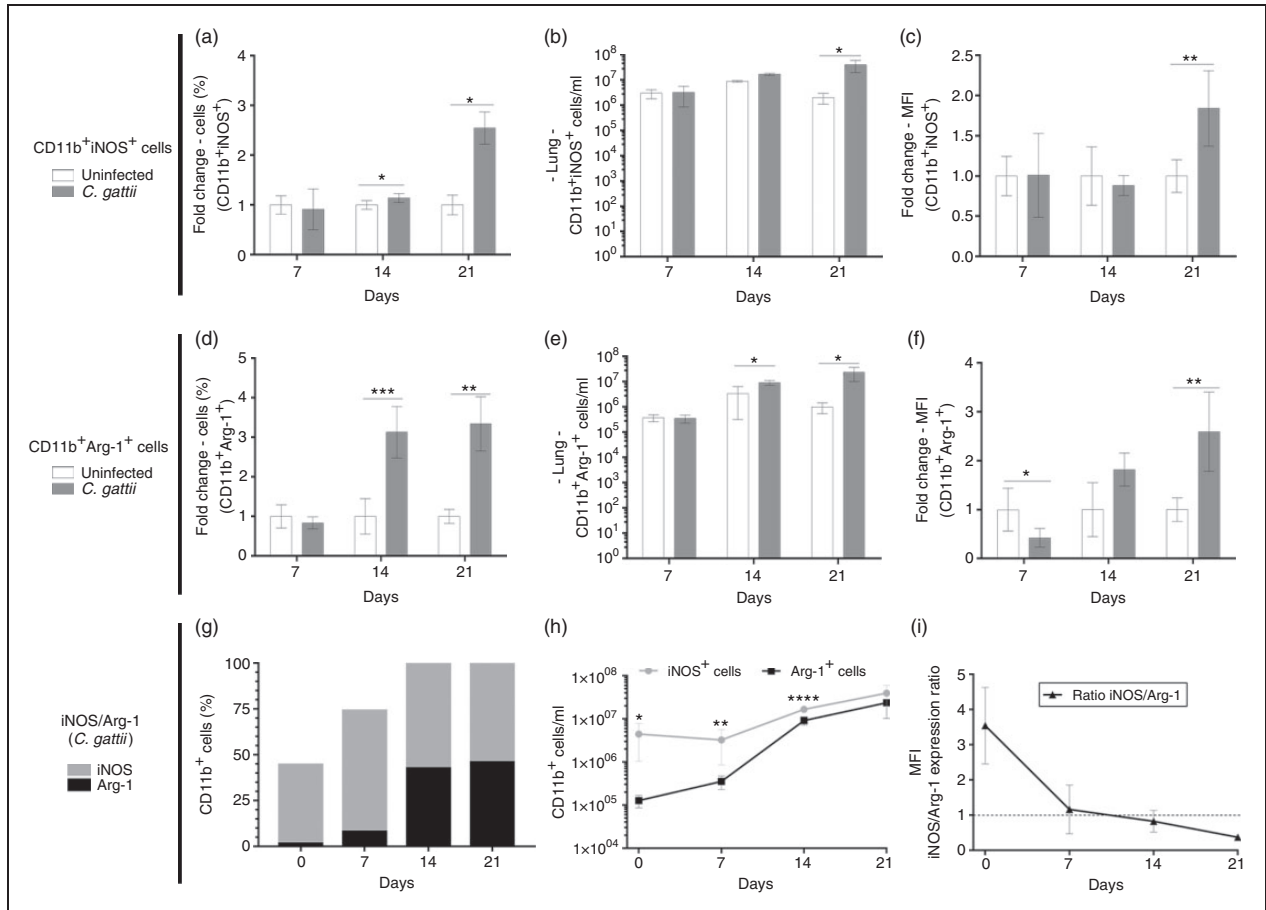


Figure 6. Phenotype of $CD11b^{+}iNOS^{+}$ and $CD11b^{+}Arg-1^{+}$ cells in the lung tissue of BALB/c infected with *C. gattii*. (a–c) $CD11b^{+}iNOS^{+}$ and $CD11b^{+}iNOS^{+}$ or (d–f) $CD11b^{+}Arg-1^{+}$ cells were quantitated by flow cytometry. Frequency, cell concentration and mean fluorescence intensity were evaluated. The fold change in (a), (c), (d) and (f) is shown as the ratio between the value from each infected mouse and the mean value of the uninfected group. (g and h) $CD11b^{+}iNOS^{+}/CD11b^{+}Arg-1^{+}$ in *C. gattii*-infected mice using the percentage and cell concentration of (a and b) $CD11b^{+}iNOS^{+}$ and (d and e) $CD11b^{+}Arg-1^{+}$ cells. (i) Mean fluorescence intensity of $CD11b^{+}iNOS^{+}$ and $CD11b^{+}Arg-1^{+}$ cells quantified by flow cytometry was used to calculate the iNOS/Arg-1 ratio. The injection of PBS alone (uninfected mice) was used in the uninfected controls. Results are expressed in percentages and represent the mean \pm SD. Differences were considered significant when * $P < 0.05$, ** $P < 0.01$ and *** $P < 0.001$ relative to uninfected controls.

infiltration of $CD11b^{+}$ cells into the pulmonary tissue after infection, with the concentration of $CD11b^{+}/Arg-1$ cells increasing over time during infection and reaching levels close to those of $CD11b^{+}/iNOS$ cells by d 21 post infection. Moreover, the iNOS/Arg-1 expression ratio fell to its lowest level at 21 d of *C. gattii* infection. The pulmonary micro-environment of infected mice had low levels of IL-10 on d 21 post infection, while the levels of pro-inflammatory cytokines did not differ during the period of *C. gattii* infection studied. Unexpectedly, the survival of iNOS KO mice was better than that of WT mice after infection with *C. gattii*, despite the iNOS KO mice having an increased pulmonary fungal burden at 14 d post infection. Thus, this study reports new features of the dynamic $CD11b^{+}iNOS^{+}/CD11b^{+}Arg-1^{+}$ cells during progression of *C. gattii* infection.

C. gattii is typically found in tropical and subtropical regions, but it has recently been found in temperate climates as well.³² It has also been reported in HIV-positive individuals residing in sub-Saharan Africa.^{33,34} Most patients with cryptococcal lung infection show symptoms such as a dry cough, dyspnoea, chest tightness and fever. However, some patients with cryptococcal pulmonary infection have more vague symptoms. So, an early diagnosis becomes a challenge.³⁵ From the *C. gattii* strains that have been studied in murine model of infection, we chose the strain R265 because of its high virulence relative to R272 and WM276 in C57BL/6 and A/JCr mice.³⁶ The infection of C57BL/6 mice with strain R265 (5×10^4 yeasts) by intra-pharyngeal aspiration was more lethal than that with *C. neoformans* strain H99. Moreover, the pulmonary fungal burden was more severe in mice infected with R265.²

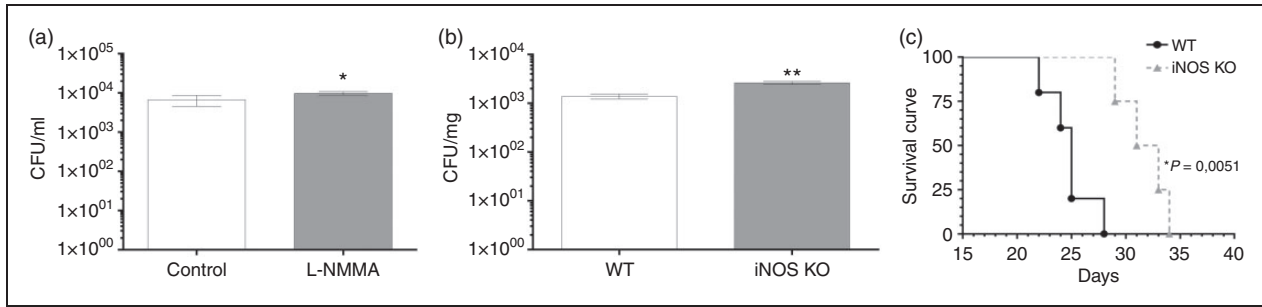


Figure 7. Pulmonary fungal burden and survival curve of iNOS KO mice infected with *C. gattii*. (a) AMJ2-C11 macrophages (5×10^5 cells/ml) were treated with L-NMMA (1 mM) or medium alone for 4 h, and these cells were infected with *C. gattii* (5×10^3 cells/ml). After 24 h, the monolayer culture was detached and combined with supernatant to quantify the growth of *C. gattii* by the CFU assay. (b and c) C57BL/6 mice (genetic background control) and iNOS KO mice were infected i.n. with 10^4 *C. gattii* yeasts. Pulmonary fungal burdens are expressed as CFU/mg organ mass and were measured after 14 d of infection. (b) The fungal burden of these mice is compared to that in C57BL/6 mice. (a and b) The results are expressed as means \pm SD (SEM). (c) For survival curves, the mortality rate was monitored daily and is expressed as a percentage. Differences were considered significant when * $P < 0.05$ and ** $P < 0.01$ relative to uninfected controls.

In this study, 100% mortality was observed by d 28 post infection in C57BL/6 mice infected with 5×10^4 yeast of *C. gattii*. Our results from intra-nasal infection of BALB/c mice with 1×10^4 yeasts of strain R265 are consistent with the C57BL/6 results. We observed that the pulmonary fungal burden increased consistently during infection, and extra-pulmonary infection was established in 100% of mice at 21 d post infection, which is also consistent with previous studies.² Conversely, we could detect *C. gattii* in the peripheral blood only after d 21 of infection in 65% of infected mice. These findings show that intra-nasal inoculation establishes extra-pulmonary infection, as has been observed with the intra-pharyngeal route of infection.

The distribution of *C. gattii* in extra-pulmonary organs prompted us to follow the serum levels of relevant biochemical parameters throughout the infection. Our results demonstrate that the biochemical parameters analysed were not strictly correlated with the progression of *C. gattii* infection in specific organs. By contrast, the relative number of neutrophils and lymphocytes was higher on d 21 post infection (Figure 2e). These findings suggest that the ability of *C. gattii* and its Ags to inhibit neutrophil migration *in vivo* and *in vitro*^{20,36} may explain normal absolute numbers of neutrophils in the blood on d 7, 14 and 21 post infection. A previous report verified the ability of *C. gattii* Ags to maintain CD4⁺ T cells in lung-draining lymph nodes at 7 and 14 d post infection.²⁰ This study is supported by our demonstration of a higher infiltrate of CD4⁺ T cells and CD8⁺ T cells in the pulmonary tissue, with a reduction of lymphocyte numbers in peripheral blood on d 21 post infection.

The protective immune response to cryptococcal infection involves adaptive immunity, particularly cell-mediated immunity, which controls *C. gattii*

infection.³⁷ The mechanism used by *C. gattii* to escape the Th1- and Th17-mediated immunity primarily involves impairment of innate immune-cell activation, blocking the development of fungus-specific Th1 and Th17 cells, compromising the DC-mediated effective response, which has been well documented.^{20,21} Consistent with this mechanism, we found a higher infiltrate of CD4⁺ T cells and CD8⁺ T cells in the lungs of infected mice after 21 d of infection (Figure 3), suggesting a delay in the development of cell-mediated immunity. In addition, the relative expression of transcripts for T-bet and ROR- γ t in the lungs of mice infected with *C. gattii* were significantly higher than those of mice infected with *C. neoformans*, indicating that *C. gattii* regulates the host adaptive immune response more strongly in the pulmonary tissue.²⁰ This modulation of the host immune response is supported by demonstration of a deficiency of *C. gattii*-infected mice to increase pulmonary pro-inflammatory cytokine levels (Figure 4). Previous studies also showed that *C. gattii* infection induced lower levels or unaltered levels of protective cytokines.^{20,36} These findings highlight the capacity of *C. gattii* infection to alter the cytokine micro-environment and to control the infiltration of T cells in the lungs, which contributes to disease progression.

In the case of *C. neoformans* infection, macrophage polarisation in the lungs from BALB/c mice infected intra-tracheally with 10^4 yeasts was altered during infection. The pulmonary macrophages were strongly M2-polarised, which was verified by high levels of Arg-1 mRNA at 1 wk post infection, while the polarisation of macrophages shifted to M1 at 3 and 4 wk following *C. neoformans* infection.³⁸ Until now, the iNOS and Arg-1 expression in the pulmonary tissue during *C. gattii* infection has not been evaluated. We infected

BALB/c mice with 10^4 *C. gattii* yeasts by the intranasal route and measured the levels of Arg-1, YM-1 and iNOS mRNA in the pulmonary tissue. We detected high levels of transcripts from M2 macrophages at wk 2 and 3 post infection, while the relative expression of the M1 marker iNOS did not predominate throughout the infection period (Figure 5). This micro-environment produced in the lungs by *C. gattii* infection led us to measure the prevalence of CD11b cells positive for iNOS and Arg-1 expression by flow cytometry. Pulmonary leucocyte analysis from *C. gattii*-infected mice revealed a prevalence of frequency and cell concentration of CD11b⁺/iNOS⁺ cells on d 7 and 14 post infection (Figure 6h). However, an increase in frequency and concentration of CD11b⁺/Arg-1⁺ cells in the lungs of *C. gattii*-infected mice occurred mainly between d 7 and 14 (Figure 6g and h). The augmentation of CD11b⁺/Arg-1⁺ cells during infection was corroborated by the iNOS/Arg-1 expression ratio within CD11b⁺ cells, which reached a low level on d 21 post infection (Figure 6). Our results demonstrate that CD11b⁺iNOS⁺/CD11b⁺Arg-1⁺ has a plasticity in the pulmonary tissue of *C. gattii*-infected mice, suggesting a critical factor in host-pathogen interaction. We believe that the prevalence of CD11b⁺/iNOS⁺ cells in the lungs of *C. gattii*-infected mice for 14 d could be caused by the host immune response, despite the inability to control pathogenesis. Previous studies showed that iNOS sourced from macrophages regulates M1 macrophage differentiation and the production of inflammatory cytokines usually produced by M1 macrophages, but this finding is not fully understood.³⁹ Therefore, the high levels of CD11b⁺/iNOS⁺ cells in the lungs of *C. gattii*-infected mice identified on d 7 may impair M1 macrophage differentiation and the production of pro-inflammatory cytokines, as verified on d 14 and 21 post infection (Figure 6). The effect of iNOS expression on the regulation of M1 macrophages produces a significant increase in CD11b⁺/Arg-1⁺ cells in the pulmonary tissue of infected mice on d 14 and 21 post infection. However, a balance in the M1/M2 macrophage ratio could prevent tissue damage. Thus, the progression of *C. gattii* infection can be favoured by the lack of a balance in CD11b⁺iNOS⁺/CD11b⁺Arg-1⁺ early in infection.

Considering that iNOS is essential for pulmonary macrophage polarisation into the M1 subtype and there is little knowledge about such polarisation during *C. gattii* infection, we investigated the fungal burden in the pulmonary tissue from iNOS KO mice. The mice lacking iNOS had a higher burden than that of WT control infected mice at d 14 post infection (Figure 7). Davis et al.³⁸ also demonstrated that M1 polarised by an IFN- γ stimulus had enhanced inhibition of *in vitro* growth of *C. neoformans*. These M1

macrophages depend strictly on iNOS to produce NO as an anti-microbial effector molecule.^{40,41} and also as an immunosuppressive molecule that mediates the apoptosis of inflammatory cells.⁴² In this context, Rossi et al.⁴¹ verified that the inhibition of iNOS *in vivo* by aminoguanidine promoted an increase in yeast burden in the lungs and decreased rat survival after *C. neoformans* infection. Furthermore, Aguirre et al.¹⁵ and Rivera et al.⁴³ demonstrated that intra-tracheal cryptococcal infection in iNOS KO mice resulted in lower survival relative to WT controls, but a lower pulmonary fungal burden was detected in the iNOS KO mice. In contrast, we found that iNOS KO mice infected with *C. gattii* had a longer survival curve relative to that of WT control mice, despite a higher pulmonary fungal burden. These findings demonstrate a divergence between survival and fungal burden, which was noted after infection with both *C. neoformans*⁴⁴ and *Candida albicans*.⁴⁵ This dissociation may be caused by factors other than fungal burden, and supporting that hypothesis, Chiapello et al.⁴² observed that the high levels of NO induced by *C. gattii* mediated the apoptosis of inflammatory cells, compromising the control of cryptococcosis. Moreover, Cánovas et al.⁴⁶ reported that the deletion of iNOS attenuated or restored the virulence of *C. neoformans*. In addition, the inhibition of ROS in macrophages impaired increased intracellular proliferation of *C. gattii*.^{24,25} Thus, our findings suggest an important role of iNOS in the pathogenesis of *C. gattii* strain R265 that may be related to the maintenance of virulence, which may be supported by the 'division of labour' hypothesised by Voelz et al.²⁵ or may be related to the effect of iNOS expression in the balance between M1 and M2 macrophages.^{8,39} The current work indicates that the effect of inhibition and lack of iNOS on progression of *C. gattii* infection should be evaluated among distinct strains of mice.

Conclusion

In conclusion, we found that intra-nasal inoculation of *C. gattii* establishes a systemic infection spreading to multiple organs, and the primary target organ of *C. gattii* had a cytokine micro-environment favouring *C. gattii* growth. The regulation of iNOS/Arg-1 expression in the pulmonary tissue is critical in *C. gattii* pathogenesis and is likely to be modulated by iNOS expression.

Acknowledgements

We thank Patrícia E Vendruscolo, Sandra M O Thomaz and Érica Vendruscolo for technical support, and Domingos Soares de Souza Filho and Adriana Sestari for expert animal care.

Declaration of conflicting interests

The author(s) declared no potential conflicts of interest with respect to the research, authorship and/or publication of this article.

Funding

The author(s) disclosed receipt of the following financial support for the research, authorship and/or publication of this article: This work was supported by the Fundação de Amparo à Pesquisa do Estado de São Paulo (Grant Nos. 2016/04877-2, 2016/10446-4, 2016/23112-7, 2016/25167-3 and 2016/03322-7), Conselho Nacional de Desenvolvimento Científico e Tecnológico (CNPq) and Fundação de Amparo à Pesquisa e Assistência (FAEPA) do Hospital das Clínicas da Faculdade de Medicina de Ribeirão Preto.

ORCID iD

Thiago Aparecido da Silva  <https://orcid.org/0000-0001-5017-6539>

References

- Rajasingham R, Smith RM, Park BJ, et al. Global burden of disease of HIV-associated cryptococcal meningitis: an updated analysis. *Lancet Infect Dis* 2017; 17: 873–881.
- Ngamskulrungrroj P, Chang Y, Sionov E, et al. The primary target organ of *Cryptococcus gattii* is different from that of *Cryptococcus neoformans* in a murine model. *MBio* 2012; 3.
- Lohmann-Matthes ML, Steinmüller C and Franke-Ullmann G. Pulmonary macrophages. *Eur Respir J* 1994; 7: 1678–1689.
- McQuiston TJ and Williamson PR. Paradoxical roles of alveolar macrophages in the host response to *Cryptococcus neoformans*. *J Infect Chemother* 2012; 18: 1–9.
- Murray PJ and Wynn TA. Protective and pathogenic functions of macrophage subsets. *Nat Rev Immunol* 2011; 11: 723–737.
- Rath M, Müller I, Kropf P, et al. Metabolism via arginase or nitric oxide synthase: two competing arginine pathways in macrophages. *Front Immunol* 2014; 5: 532.
- Giordano D, Li C, Suthar MS, et al. Nitric oxide controls an inflammatory-like Ly6C(hi)PDCA1+ DC subset that regulates Th1 immune responses. *J Leukoc Biol* 2011; 89: 443–455.
- Lu G, Zhang R, Geng S, et al. Myeloid cell-derived inducible nitric oxide synthase suppresses M1 macrophage polarization. *Nat Commun* 2015; 6: 6676.
- Rodriguez PC, Ochoa AC and Al-Khami AA. Arginine metabolism in myeloid cells shapes innate and adaptive immunity. *Front Immunol* 2017; 8: 93.
- Mao K, Chen S, Chen M, et al. Nitric oxide suppresses NLRP3 inflammasome activation and protects against LPS-induced septic shock. *Cell Res* 2013; 23: 201–212.
- Mishra BB, Rathinam VA, Martens GW, et al. Nitric oxide controls the immunopathology of tuberculosis by inhibiting NLRP3 inflammasome-dependent processing of IL-1 β . *Nat Immunol* 2013; 14: 52–60.
- Yakovlev VA, Barani IJ, Rabender CS, et al. Tyrosine nitration of IkappaBalpha: a novel mechanism for NF-kappaB activation. *Biochemistry* 2007; 46: 11671–11683.
- Ganguly D, Haak S, Sisirak V, et al. The role of dendritic cells in autoimmunity. *Nat Rev Immunol* 2013; 13: 566–577.
- Burrack KS and Morrison TE. The role of myeloid cell activation and arginine metabolism in the pathogenesis of virus-induced diseases. *Front Immunol* 2014; 5: 428.
- Aguirre KM and Gibson GW. Differing requirement for inducible nitric oxide synthase activity in clearance of primary and secondary *Cryptococcus neoformans* infection. *Med Mycol* 2000; 38: 343–353.
- Chen GH, McDonald RA, Wells JC, et al. The gamma interferon receptor is required for the protective pulmonary inflammatory response to *Cryptococcus neoformans*. *Infect Immun* 2005; 73: 1788–1796.
- Wormley FL Jr, Perfect JR, Steele C, et al. Protection against cryptococcosis by using a murine gamma interferon-producing *Cryptococcus neoformans* strain. *Infect Immun* 2007; 75: 1453–1462.
- Murdock BJ, Huffnagle GB, Olszewski MA, et al. Interleukin-17A enhances host defense against cryptococcal lung infection through effects mediated by leukocyte recruitment, activation, and gamma interferon production. *Infect Immun* 2014; 82: 937–948.
- Wozniak KL, Hardison SE, Kolls JK, et al. Role of IL-17A on resolution of pulmonary *C. neoformans* infection. *PLoS One* 2011; 6: e17204.
- Angkasekwinai P, Sringkarin N, Supasorn O, et al. *Cryptococcus gattii* infection dampens Th1 and Th17 responses by attenuating dendritic cell function and pulmonary chemokine expression in the immunocompetent hosts. *Infect Immun* 2014; 82: 3880–3890.
- Huston SM, Ngamskulrungrroj P, Xiang RF, et al. *Cryptococcus gattii* capsule blocks surface recognition required for dendritic cell maturation independent of internalization and antigen processing. *J Immunol* 2016; 196: 1259–1271.
- Herkert PF, Dos Santos JC, Hagen F, et al. Differential *in vitro* cytokine induction by the species of *Cryptococcus gattii* complex. *Infect Immun* 2018; 86.
- Ikeda-Dantsuji Y, Ohno H, Tanabe K, et al. Interferon- γ promotes phagocytosis of *Cryptococcus neoformans* but not *Cryptococcus gattii* by murine macrophages. *J Infect Chemother* 2015; 21: 831–836.
- Ma H, Hagen F, Stekel DJ, et al. The fatal fungal outbreak on Vancouver Island is characterized by enhanced intracellular parasitism driven by mitochondrial regulation. *Proc Natl Acad Sci U S A* 2009; 106: 12980–12985.
- Voelz K, Johnston SA, Smith LM, et al. ‘Division of labour’ in response to host oxidative burst drives a fatal *Cryptococcus gattii* outbreak. *Nat Commun* 2014; 5: 5194.

26. Almeida F, Wolf JM, Da Silva TA, et al. Galectin-3 impacts *Cryptococcus neoformans* infection through direct antifungal effects. *Nat Commun* 2017; 8: 1968.
27. Oliveira Brito PKM, Gonçalves TE, Fernandes FF, et al. Systemic effects in naïve mice injected with immunomodulatory lectin ArtinM. *PLoS One* 2017; 12: e0187151.
28. Da Silva TA, Roque-Barreira MC, Casadevall A, et al. Extracellular vesicles from *Paracoccidioides brasiliensis* induced M1 polarization *in vitro*. *Sci Rep* 2016; 6: 35867.
29. Da Silva TA, Zorzetto-Fernandes ALV, Cecilio NT, et al. CD14 is critical for TLR2-mediated M1 macrophage activation triggered by N-glycan recognition. *Sci Rep* 2017; 7: 7083.
30. Freitas MS, Oliveira AF, Da Silva TA, et al. Paracoccin induces M1 polarization of macrophages via interaction with TLR4. *Front Microbiol* 2016; 7: 1003.
31. Zaynagetdinov R, Sherrill TP, Kendall PL, et al. Identification of myeloid cell subsets in murine lungs using flow cytometry. *Am J Respir Cell Mol Biol* 2013; 49: 180–189.
32. Caballero Van Dyke MC and Wormley FL Jr. A call to arms: quest for a cryptococcal vaccine. *Trends Microbiol* 2018; 26: 436–446.
33. Hagen F, Colom MF, Swinne D, et al. Autochthonous and dormant *Cryptococcus gattii* infections in Europe. *Emerg Infect Dis* 2012; 18: 1618–1624.
34. Litvintseva AP, Thakur R, Reller LB, et al. Prevalence of clinical isolates of *Cryptococcus gattii* serotype C among patients with AIDS in Sub-Saharan Africa. *J Infect Dis* 2005; 192: 888–892.
35. Skolnik K, Huston S and Mody CH. Cryptococcal lung infections. *Clin Chest Med* 2017; 38: 451–464.
36. Cheng PY, Sham A and Kronstad JW. *Cryptococcus gattii* isolates from the British Columbia cryptococcosis outbreak induce less protective inflammation in a murine model of infection than *Cryptococcus neoformans*. *Infect Immun* 2009; 77: 4284–4294.
37. McDermott AJ and Klein BS. Helper T-cell responses and pulmonary fungal infections. *Immunology* 2018; 155: 155–163.
38. Davis MJ, Tsang TM, Qiu Y, et al. Macrophage M1/M2 polarization dynamically adapts to changes in cytokine microenvironments in *Cryptococcus neoformans* infection. *MBio* 2013; 4: e00264-13.
39. Xue Q, Yan Y, Zhang R, et al. Regulation of iNOS on immune cells and its role in diseases. *Int J Mol Sci* 2018; 19.
40. Gonzalez A, de Gregori W, Velez D, et al. Nitric oxide participation in the fungicidal mechanism of gamma interferon-activated murine macrophages against *Paracoccidioides brasiliensis* conidia. *Infect Immun* 2000; 68: 2546–2552.
41. Rossi GR, Cervi LA, García MM, et al. Involvement of nitric oxide in protecting mechanism during experimental cryptococcosis. *Clin Immunol* 1999; 90: 256–265.
42. Chiapello LS, Baronetti JL, Garro AP, et al. *Cryptococcus neoformans* glucuronoxylomannan induces macrophage apoptosis mediated by nitric oxide in a caspase-independent pathway. *Int Immunol* 2008; 20: 1527–1541.
43. Rivera J, Mukherjee J, Weiss LM, et al. Antibody efficacy in murine pulmonary *Cryptococcus neoformans* infection: a role for nitric oxide. *J Immunol* 2002; 168: 3419–3427.
44. Feldmesser M and Casadevall A. Effect of serum IgG1 to *Cryptococcus neoformans* glucuronoxylomannan on murine pulmonary infection. *J Immunol* 1997; 158: 790–799.
45. Bulawa CE, Miller DW, Henry LK, et al. Attenuated virulence of chitin-deficient mutants of *Candida albicans*. *Proc Natl Acad Sci U S A* 1995; 92: 10570–10574.
46. Cánovas D, Marcos JF, Marcos AT, et al. Nitric oxide in fungi: is there NO light at the end of the tunnel? *Curr Genet* 2016; 62: 513–518.